

Mullite formation from non-crystalline precursors

H. SCHNEIDER

German Aerospace Research Establishment (DLR), Materials Research Institute,
Linder Höhe D-5000 Köln 90, Postfach 906058 Germany

L. MERWIN, A. SEBALD

Bayrisches Geoinstitut, University of Bayreuth, D-8580 Bayreuth, Germany

X-ray diffraction, differential thermal analysis, and ^{29}Si and ^{27}Al MAS NMR spectroscopy were used to characterize the formation of mullite from non-crystalline precursors. The precursors were produced by the sol-gel route from organic starting compounds (SGM), and by co-precipitation of inorganic starting materials (CM). There is NMR evidence that both types of mullite precursor consist of Si-O and Al-O tetrahedra, and of Al-O octahedra. Furthermore, fivefold-coordinated Al-O polyhedra, or alternatively strongly distorted Al-O tetrahedra, do occur in the precursors. SGM and CM precursors transform to mullite in multi-step reactions with intermediate formation of $\gamma\text{-Al}_2\text{O}_3$, and a non-crystalline nearly pure SiO_2 phase. The $\gamma\text{-Al}_2\text{O}_3$ compound has a highly distorted spinel structure, and may contain some minor amount of Si. The diffusion-controlled decomposition of the precursors to $\gamma\text{-Al}_2\text{O}_3 + \text{SiO}_2$ at low temperature ($\leq 1000^\circ\text{C}$) suggests that the precursors are diphasic, consisting of nanometre-sized, long-range-disordered Al_2O_3 - and SiO_2 -rich domains. The reaction of $\gamma\text{-Al}_2\text{O}_3 + \text{SiO}_2$ above about 1000°C initially produces Al_2O_3 -rich mullite. This is explained by a possible nucleation of mullite on the surfaces of $\gamma\text{-Al}_2\text{O}_3$ crystallites. The gradual transformation of the unstable, low-temperature (≥ 1000 to $\leq 1400^\circ\text{C}$) Al_2O_3 -rich mullites to the stable high-temperature ($\geq 1400^\circ\text{C}$) 3/2-type mullites ($3\text{Al}_2\text{O}_3 \cdot 2\text{SiO}_2$) is essentially controlled by the annealing temperatures, whereas annealing times play a minor role.

1. Introduction

Mullite ceramics are resistant against chemical attack, especially under oxidizing conditions. Furthermore, mullite matrix materials have low thermal expansion coefficients and are characterized by very low thermal conductivity and excellent creep resistance (see articles in Somiya *et al.* [1]). The outstanding thermal properties of mullite and mullite-matrix composites probably explain the extensive current interest in mullite ceramics, despite the relatively low mechanical strength of the materials at room temperature.

Excellent methods of producing high-performance mullite are the sol-gel and co-precipitation techniques which use Al- and Si-containing solutions as starting materials. The methods have the advantage that the starting solutions can be homogeneously admixed on a nearly molecular scale. Furthermore, mullite crystallization and sintering temperatures are lowered significantly with respect to processes occurring in $\text{Al}_2\text{O}_3\text{-SiO}_2$ powder mixtures. Although sol-gel and co-precipitation produced powders allow the production of very homogeneous, dense, and glass-free mullite ceramics, the techniques, however, have their drawbacks. The microstructures and associated mechanical properties of these ceramics are highly dependent on minor changes in reaction conditions. Hydrolytic

decomposition of the starting compounds, heating velocities and reaction atmospheres seem to play a major role. These variables in turn strongly control the microstructural development of the ceramic. A detailed knowledge of the structural long- and short-range-order of the non-crystalline precursors, and information on the mechanisms and kinetics of mullite crystallization, therefore, are of extreme importance. This knowledge could help to control the mullite formation process, and using this knowledge one could possibly improve the materials' properties.

2. Experimental procedure

The chemical composition of reference samples SGM and CM, which were annealed at 1650°C for 15 h, was determined with a computer-controlled sequential X-ray fluorescence spectrometer (XFA, Rigaku).

The powder X-ray diffraction (XRD) studies were carried out at room temperature with a computer-controlled Siemens D500 powder diffractometer (CuK_α radiation). The diffractograms were recorded in the 5 to $70^\circ 2\theta$ -range in the step-scan mode ($5\text{ s}/0.01^\circ, 2\theta$). Lattice constants and cell volumes were refined with a least-squares procedure using 25 strong and

medium reflections, with silicon ($a = 0.543088(4)$ nm) as an internal standard.

Differential thermal analyses (DTA) and thermogravimetric (TG) measurements were performed with a computer-controlled Netzsch STA 409 apparatus (sensitivity for DTA: 50 μ V, TG: 50 mg). About 70 mg of the samples and of the reference material (fired kaolinite), respectively, were heated up in Pt crucibles, with a constant heating rate of 10 K min^{-1} . All DTA and TG runs were carried out in an air atmosphere.

All ^{27}Al and ^{29}Si magic-angle spinning nuclear magnetic resonance (MASNMR) spectra were obtained on a Bruker MSL 300 NMR spectrometer, using 4 and 7 mm double-bearing probes, respectively. Spinning rates were 4 kHz (^{29}Si) and 8–12 kHz (^{27}Al). ^{29}Si chemical shifts are given with respect to external TMS using Q_8M_8 [2] as a secondary solid reference. ^{27}Al chemical shifts are given with respect to an external aqueous AlCl_3 solution; the ^{27}Al shifts are not corrected for secondary quadrupolar effects. Operating conditions were as follows:

^{29}Si : 2 μ s (36°) pulses, 30 s relaxation delay,

650–2100 transients accumulated.

^{27}Al : 1 μ s ($\text{TC}(\pi)/6$) pulses, 1 s relaxation delay,

500–2000 transients accumulated.

These conditions were checked and found to be satisfactory with respect to preventing saturation and non-selective excitation. The spectra were processed without exponential line broadening or resolution enhancement.

3. Sample preparation

3.1. Sample materials

For sol-gel materials (SGM), tetraethyl orthosilicate (TEOS) $\text{Si}(\text{OC}_2\text{H}_5)_4$ and aluminium butylate $\text{Al}(\text{OCH}(\text{CH}_3)\text{C}_2\text{H}_5)_3$ (both from Merck) were used for the mullite syntheses. Both compounds were admixed at room temperature in proportions corresponding to 72 wt % Al_2O_3 (60 mol % Al_2O_3) and 28 wt % SiO_2 (40 mol % SiO_2). Other compositions con-

taining Al_2O_3 or SiO_2 in excess were also prepared. However, these mixtures were unfavourable in producing final mullites of poor crystallinity or because Al_2O_3 was present as an additional crystalline phase. Prior to the homogenization of the starting liquids some isopropanol ($\text{C}_3\text{H}_7\text{OH}$) was added. The drop-by-drop addition of water produced a homogeneous, white gel. This gel was heat-treated in order to evaporate the excess water, and was then dried at 110 $^\circ\text{C}$.

For co-precipitated materials (CM) the starting material, which was provided by Hüls Co. (Marl, FRG), was synthesized by co-precipitation of sodium aluminate and silica sol at $\text{pH} = 7$, with H_2SO_4 , at about 50 $^\circ\text{C}$. The starting materials were admixed in proportions corresponding to 72 wt % Al_2O_3 (60 mol % Al_2O_3) and 28 wt % Al_2O_3 (40 mol % Al_2O_3) as in the case of the sol-gel materials.

3.2. Annealing experiments

SGM and CM samples were annealed at temperatures between 600 and 1650 $^\circ\text{C}$ in a laboratory chamber furnace in air atmosphere. Details of the annealing procedure are given in Table I.

4. Results

4.1. X-ray diffractometry

Samples SGM and CM 600 to 800 (Table I) are X-ray amorphous. Sol-gel samples SGM 900 to 1100 and co-precipitated samples CM 900 to 1100 both contain γ - Al_2O_3 and mullite, though γ - Al_2O_3 is predominant in the SGM materials, while mullite is the major phase in CM samples. Samples SGM 1100 and CM 1100 both contain some small amount of cristobalite. SGM and CM samples heat-treated at 1400 and 1650 $^\circ\text{C}$, respectively, are single-phase mullite. γ - Al_2O_3 and mullite produced at low temperature display broadened X-ray reflections of low intensity, which are indicative of intensive structural disorder and of small-diameter crystallites.

The lattice constants of low-temperature mullites SGM and CM 1000 correspond to those of Al_2O_3 -rich

TABLE I Annealing experiments carried out on sol-gel (SGM) and co-precipitated (CM) materials

Annealing temperature ($^\circ\text{C}$)	Sol-gel materials			Co-precipitated materials		
	Sample key	Duration of annealing (h)	Methods of characterization	Sample key	Duration of annealing (h)	Methods of characterization
600	SGM 600	15	XRD, NMR	CM 600	15	XRD, NMR
700	SGM 700	15	XRD, NMR	CM 700	15	XRD, NMR
800	SGM 800	15	XRD, NMR	CM 800	15	XRD, NMR
900	SGM 900	15	XRD, NMR	CM 900	15	XRD, NMR
1000	SGM 1000	15	XRD, NMR	CM 1000	15	XRD, NMR
1050	—	—	—	CM 1050	120	XRD
1100	SGM 1100	15	XRD, NMR	CM 1100	15	XRD, NMR
1150	—	—	—	CM 1150	120	XRD
1250	—	—	—	CM 1250	120	XRD
1400	SGM 1400	15	XRD, NMR	CM 1400	15	XRD, NMR
1650	SGM 1650	15	XRD, NMR	CM 1650	15	XRD, NMR

XRD: X-ray diffraction, NMR: ^{29}Si MAS NMR and ^{27}Al MAS NMR.

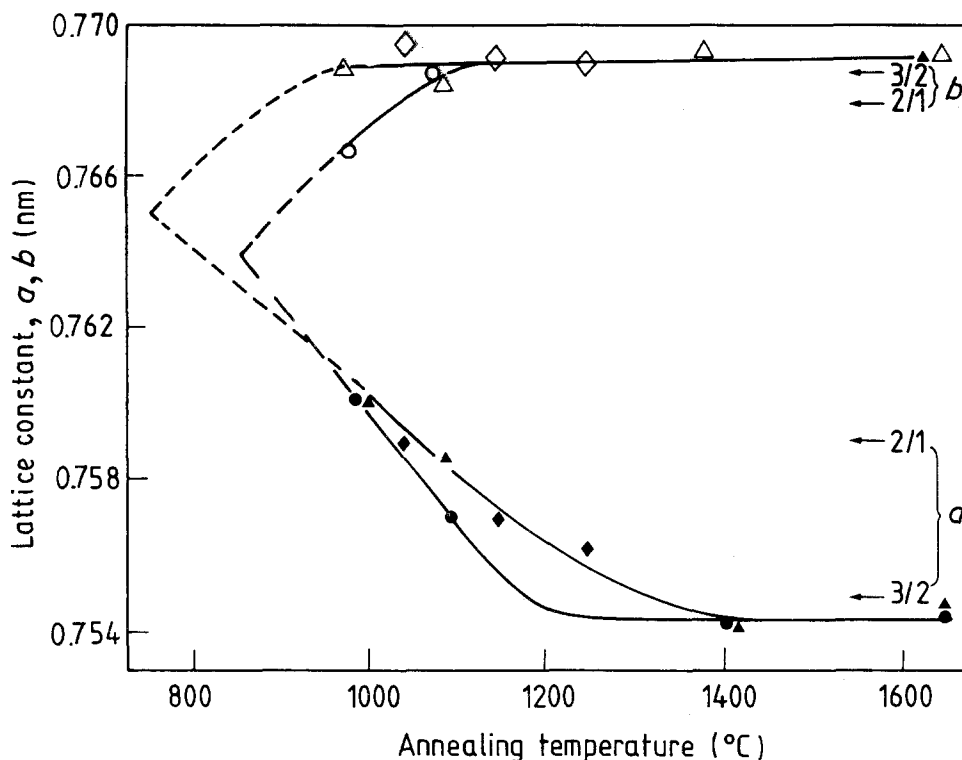


Figure 1 Lattice constants a and b of mullites produced from SGM and CM precursors (Table I). Annealing experiments were performed at 1000, 1050, 1100, 1150, 1250, 1400, and 1650 °C. SGM mullite annealed for 15 h: (●) a , (○) b . CM mullite annealed for 15 h: (▲) a , (△) b . CM mullite annealed for 120 h: (◆) a , (◇) b . The c lattice constants (not shown here) slightly increase from about 0.2880 nm at low temperature (samples SGM 1000 and CM 1000) to about 0.2884 nm at high temperature (samples SGM 1650 and CM 1650, Table I). Lattice constants a and b characterized by arrows refer to those of $3\text{Al}_2\text{O}_3 \cdot 2\text{SiO}_2$ mullite (3/2) and of $2\text{Al}_2\text{O}_3 \cdot \text{SiO}_2$ mullite (2/1), as indicated.

mullites. Lattice constants a decrease with increasing annealing temperature, while the b constants slightly increase, and c does not change significantly (Fig. 1). The lattice constants of SGM and CM mullites 1400 and 1650 are very close to those of stoichiometric 3/2-mullite ($3\text{Al}_2\text{O}_3 \cdot 2\text{SiO}_2$). Lattice constants of CM mullites obtained by extended annealing experiments (Table I) fit well into the temperature-dependent curves of the short time runs. The formation of Al_2O_3 -rich mullites from sol-gel precursors at relatively low temperature and their gradual temperature-dependent transformation to stable 3/2-mullite is stressed by other publications [3–6].

4.2. Differential thermal analysis

Heating DTA curves of the SGM sol-gel materials display broad endothermic peaks near 135 and 229 °C, a sharp exotherm of high intensity at 988 °C, and an additional weak exotherm signal near 1253 °C. The DTA pattern of the co-precipitated CM material is similar to that of the SGM sample with endotherms near 135 and 219 °C, and a major exotherm at about 988 °C. However, the 988 °C signal of the CM material is much broader and of lower intensity than that in the SGM spectrum. The 988 °C peak furthermore displays a shoulder at about 970 °C, which is associated with a weight loss. The CM DTA spectrum shows no exotherm at 1250 °C (Fig. 2a and b). The high-temperature branch of the DTA curve of SGM material is remarkably similar to those reported for xerogels [7]

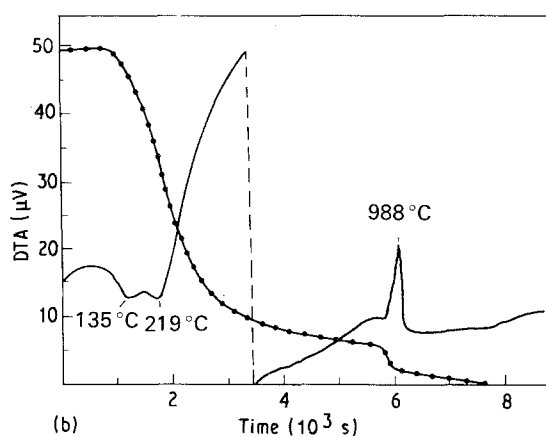
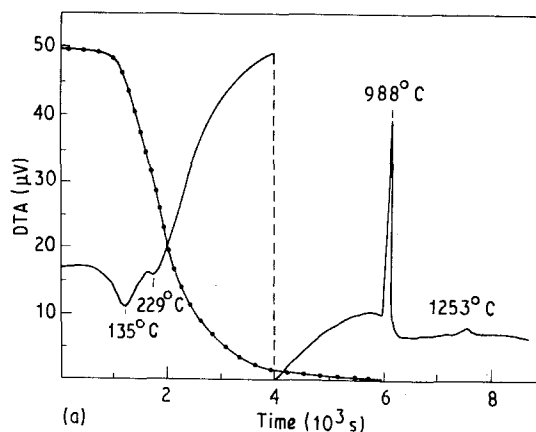


Figure 2 (—) DTA and (●) TG curves of (a) sol-gel (SGM) and (b) co-precipitated (CM) starting materials.

and for the high-temperature products of the metakaolinite–mullite reaction sequence [8, 9]. In the metakaolinite–mullite DTA an exotherm was described near 960 °C, which was attributed to mullite and γ - Al_2O_3 formation and to liberation of a non-crystalline SiO_2 -rich phase. The 1250 °C signal was assigned to the reaction of γ - Al_2O_3 with amorphous SiO_2 to form mullite. The similarity of DTA patterns is less significant for co-precipitated CM samples since the 1250 °C signal is absent. This may be explained by

the low γ - Al_2O_3 content in this sample, which does not give rise to a significant 1250 °C reaction process.

4.3. NMR spectroscopy

4.3.1. ^{29}Si MAS NMR

The ^{29}Si MAS NMR spectra of precursors SGM 600 to SGM 800, and CM 600 to CM 700 (Fig. 3a and b), contain peak maxima near -92 and -95 p.p.m.,

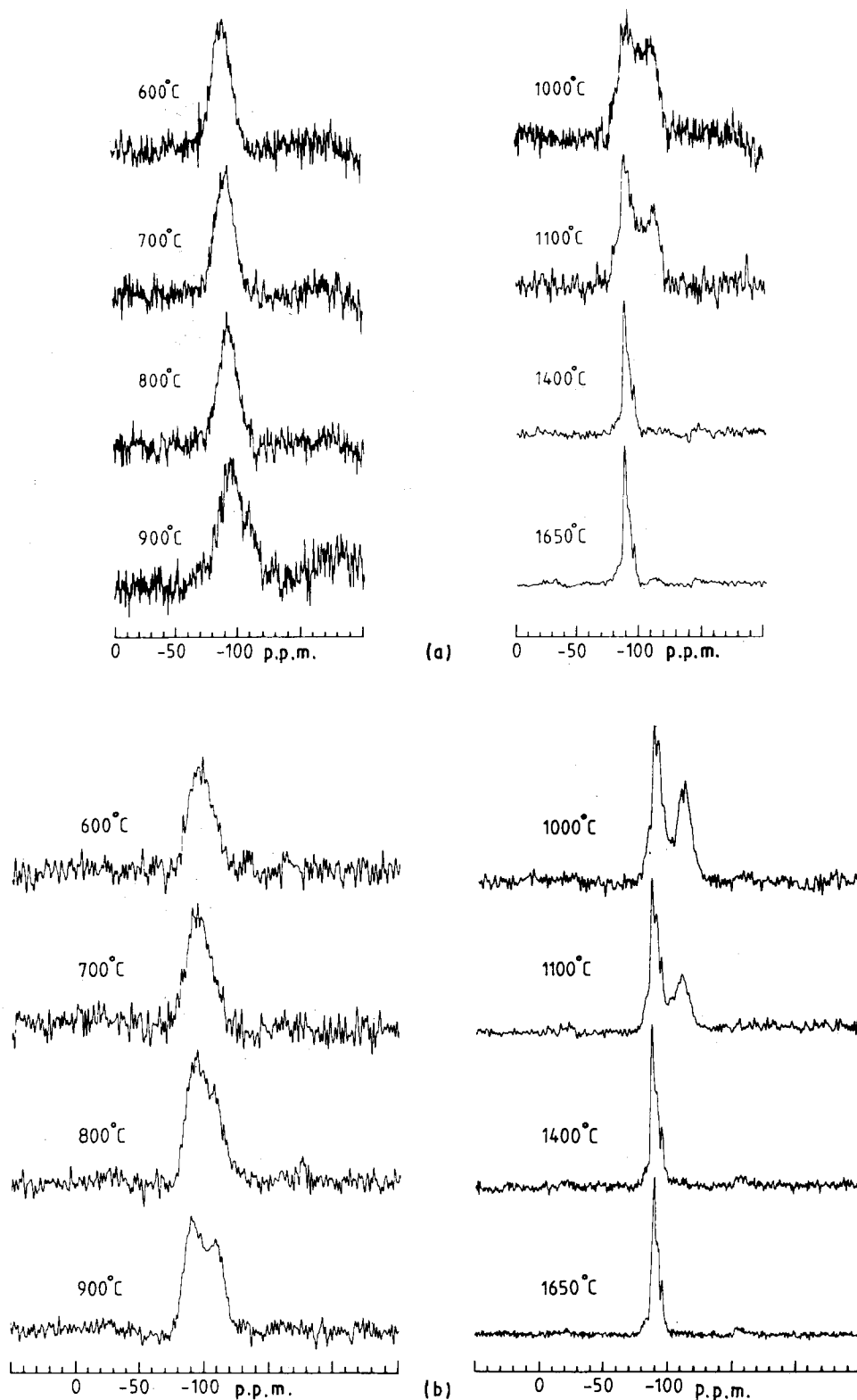


Figure 3 ^{29}Si MAS NMR spectra of mullite precursor materials heat-treated at different temperatures (Table I); (a) sol-gel material (SGM) (b) co-precipitated material (CM). Details and experimental conditions are given in the text.

respectively. According to the correlation of Engelhardt and Michel [2] this indicates the occurrence of Q^3 [$Si(OSi)_3O^-$] units, or a silicon environment in the Si(4Al)/Si(3Al) region. If the latter assignment is correct, CM precursor phases contain less Al as next-nearest neighbours than SGM precursors.

We do not believe that the Si sites in the precursors correspond to those in sillimanite ($Al_2O_3 \cdot SiO_2$) (resonance at -87 p.p.m.) as was suggested for roller-quenched glasses of the $Al_2O_3-SiO_2$ sequence (resonance at -90 p.p.m., [10]).

At the low annealing temperatures both samples, SGM and CM, display broad chemical shift distributions, which should be explained by a large variety of overlapping signals, due to the occurrence of geometrically slightly different structural SiO_4 units. However, while SGM 600 to SGM 800 precursors produce fairly symmetrical ^{29}Si resonances, those of the corresponding CM 600 to CM 800 precursors have an asymmetrical shape with a shoulder towards lower frequencies (more negative chemical shifts). The shapes of the CM resonances are interpreted as being due to the overlapping of a broad resonance similar to that of SGM precursors near -95 p.p.m., and another broad resonance of lower intensity near -110 p.p.m. We believe that the observation is indicative for a separation into SiO_2 -poorer (≈ -90 p.p.m.) and SiO_2 -richer domains (≈ -110 p.p.m.) in CM precursors CM 600 to CM 800, while only " SiO_2 -poor" domains (≈ -90 p.p.m.) seem to occur in precursors SGM 600 to SGM 800. Systematic studies are being carried out in order to explain these phenomena.

Above $800^\circ C$ the split of the ^{29}Si resonance into resonances near -90 and -110 p.p.m. appears in both materials. Thereby the maximum of the formation of the SiO_2 -rich phase of CM samples occurs at lower temperatures than that of SGM samples (Fig. 3a and b). This may be explained by the presence of SiO_2 -rich domains in the low-temperature CM precursors but not in corresponding SGM samples. At temperatures above $1100^\circ C$ the SiO_2 -rich phase disappears, probably due to a reaction with Al_2O_3 -rich mullite to form stoichiometric mullite (see Section 4.1).

The ^{29}Si spectra of samples SGM 900 to SGM 1100 and CM 1000 to CM 1100 display shoulders of low intensity near -80 p.p.m. This could indicate that the $\gamma-Al_2O_3$ formed out of the precursors is not really pure Al_2O_3 but contains some Si [11, 12]. However, because of the high amount of the SiO_2 -rich phase coexisting with $\gamma-Al_2O_3$ we believe that $\gamma-Al_2O_3$ incorporates only minor amounts of Si, and therefore does not have the composition suggested by Chakravorty and Ghosh [13].

Above $\geq 1400^\circ C$ SGM and CM samples become essentially indistinguishable by means of ^{29}Si MAS NMR: they display sharp peaks near -87 and -94 p.p.m., and shoulders near -90 p.p.m. which are typical for mullite [14].

4.3.2. ^{27}Al MAS NMR

The ^{27}Al MAS NMR spectra (Fig. 4a and b) of sam-

ples SGM 600 to SGM 800 and CM 600 to CM 900 display broad resonances around 2 p.p.m., 30 p.p.m., and in the 58–66 p.p.m. region. The latter resonances can clearly be assigned to tetrahedrally coordinated Al, while the low-frequency resonances at ≈ 2 p.p.m. arise from Al in octahedral coordination. Resonances near 30 p.p.m. have previously been assigned to fivefold-coordinated Al [2, 10, 14, 15]. However, the term "fivefold-coordinated Al" may have to be used with caution, as it is very much a matter of opinion under what circumstances one should speak of fivefold coordination. Perhaps it would be wiser to use the less precise but more descriptive term "strongly distorted tetrahedral Al sites with excess oxygen neighbours". Qualitatively the ^{27}Al MAS spectra for this temperature regime support the findings from the respective ^{29}Si MAS spectra: clearly we deal with samples which are amorphous on an NMR scale, i.e. both short- and long-range orders are poor.

Above 800 to $900^\circ C$ the 30 p.p.m. resonances decrease strongly in intensity, and are no longer found at $1000^\circ C$. Simultaneously the octahedral Al resonances of SGM samples shift towards ≈ 8 p.p.m., while the tetrahedral Al resonances move to ≈ 70 p.p.m. The great similarity of these spectra with those of kaolinite heat-treated at $1000^\circ C$ suggests that their appearance is essentially due to the presence of a $\gamma-Al_2O_3$ phase [15]. Corresponding CM samples display ^{27}Al MAS NMR spectra similar to that of mullite, though signals are broadened and have no fine structure.

Above $1100^\circ C$ both CM and SGM samples show what might be called typical mullite ^{27}Al spectra (resonances at 62, 45 and -5 p.p.m.). The patterns of these ^{27}Al spectra as a function of temperature above $1000^\circ C$ indicate that stoichiometric mullite formation is a gradual process (see also [14]). It should be noted that, just as for the respective ^{29}Si MAS spectra, CM and SGM samples become indistinguishable by means of NMR at temperatures above $1400^\circ C$.

Comparing the temperature-dependent changes in the ^{29}Si MAS spectra of CM and SGM samples with changes observed in their respective ^{27}Al MAS spectra, small but possibly significant differences are found: in the ^{29}Si MAS spectra the onset of "crystallization" for the CM material is observed at somewhat lower temperatures than for the SGM material ($\leq 800^\circ C$ versus $\geq 800^\circ C$). In the ^{27}Al MAS spectra, however, the reverse situation is found. At $900^\circ C$ the CM material still displays the broad "amorphous" resonances, while for the SGM material these resonances have already collapsed into the intermediate reaction-type resonances. However, far-reaching interpretation will certainly need further independent experimental proof, since at this point genuine problems with the high-resolution solid-state NMR properties of quadrupolar nuclei in amorphous materials come into play: though careful ^{27}Al NMR data are acquired, we have little or no control over whether we measure spectra which can be considered truly representative for the bulk of the sample. The situation is different for spin-1/2 nuclei like ^{29}Si , where carefully chosen and checked operating conditions lead to reliable and directly interpretable spectra.

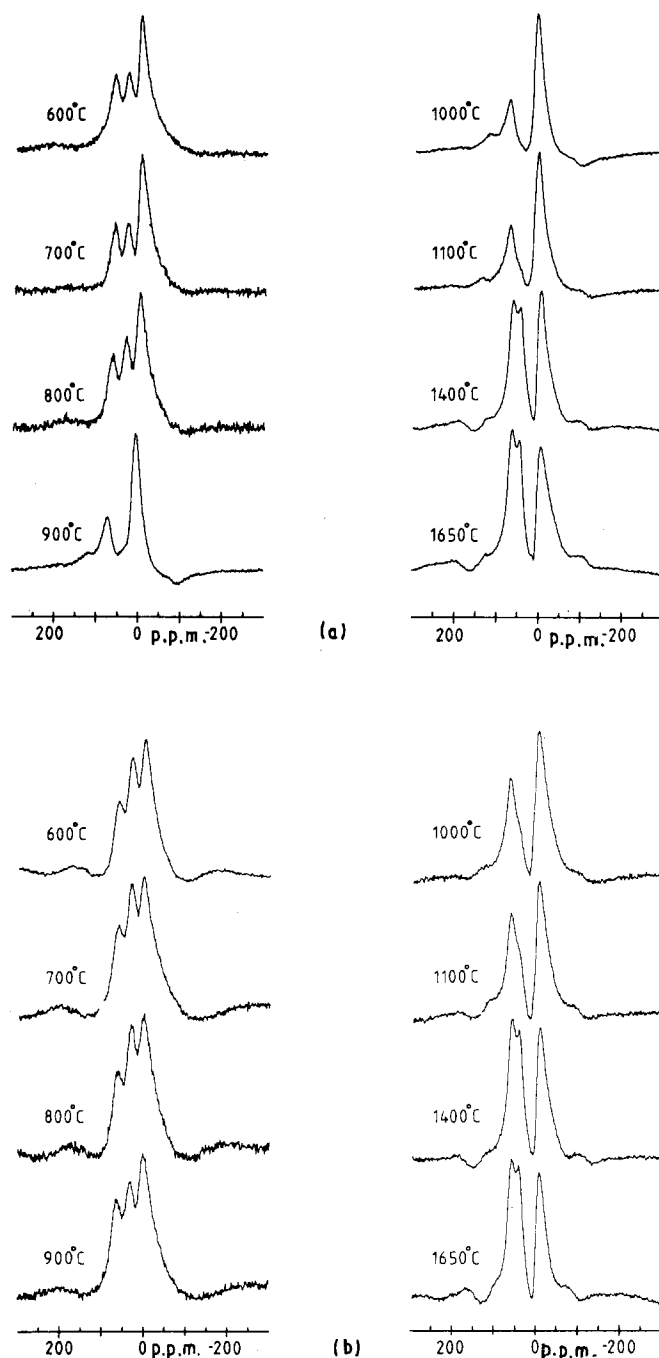


Figure 4 ^{27}Al MAS NMR spectra of mullite precursor materials heat-treated at different temperatures (Table I): (a) sol-gel material (SGM), (b) co-precipitated material (CM). Details and experimental conditions are given in the text.

There is no way out of this “quadrupolar dilemma” using conventional MAS NMR techniques [16], especially not in a case such as we have here, where it seems impossible to add some crystalline ^{27}Al -containing material as a quantitation aid – all possible ^{27}Al resonance positions are used up by the sample itself. This also puts the following observation in perspective: at first glance the ^{27}Al MAS spectra appear more dramatically different for SGM and CM materials than the respective ^{29}Si MAS spectra. But – as we can see from the ^{29}Si MAS spectra – we cannot expect the same degree and type of “non-crystallinity” or “disorder” for these two bulk-chemically equivalent types of precursor materials. Therefore, we have no guarantee that the ^{27}Al MAS spectra of the SGM and

CM materials, which suffer from the same distortions, will show (or rather: not show) the same invisible Al. Especially at our moderate magnetic field strength of 7 T it is most likely that, in the ^{27}Al spectra, sites with minor distortions will be emphasized at the expense of more distorted ^{27}Al sites.

With respect to the ^{27}Al MAS NMR spectra we feel very strongly that the interpretation must be strictly qualitative – and certainly not beyond what has been described in the above paragraph. To us, the only acceptable strategy will have to rely heavily on the more favourable (i.e. more controllable) properties of the spin-1/2 nuclei, even if data acquisition for these nuclei is far more time-consuming. ^{27}Al MAS NMR data for such amorphous materials should be used

merely as experimental support. Any further interpretation of conventional ^{27}Al data must be accompanied by strong independent experimental support from other spectroscopic or diffraction techniques. The only other potential escape from the “quadrupolar problem” in amorphous materials could be offered by unrealistically high magnetic field strengths of several hundred Tesla, or – more realistically – will eventually emerge from more sophisticated experimental NMR techniques, e.g. double-angle rotation experiments [17–20].

5. Discussion

Sol-gel and co-precipitation derived precursors in the system Al_2O_3 – SiO_2 are highly metastable systems which can be either single-phase or alternatively diphasic, depending on the degree of Al_2O_3 and SiO_2 mixing. The crystallization temperatures of the precursors are controlled by the chemical composition of the material, by the short- and long-range order of the phases (“structure”), and by the size and shape of particles.

NMR spectroscopic data imply that SGM and CM precursors consist of fourfold-coordinated Si–O tetrahedra, fourfold-coordinated Al–O tetrahedra, and sixfold-coordinated Al–O octahedra. The NMR signal, which has been assigned as being due to fivefold-coordinated Al–O polyhedra [10] should better be attributed to strongly distorted Al–O tetrahedra with close next O neighbours. The broad NMR resonances and the lack of X-ray reflections indicate a variety of highly distorted, very small O–Si–O–Al–O- or SiO_2 - and Al_2O_3 -rich units in both precursors. There is evidence that the Si site distribution in the SGM precursors is fairly homogeneous, while CM precursors may contain two types of SiO_2 -rich units, one being slightly richer in SiO_2 than the other. The separation of the SiO_2 -rich units into two groups of different chemical composition becomes more significant with increasing temperature.

Both precursors, SGM and CM, transform to mullite in a multi-step reaction with intermediate formation of a γ - Al_2O_3 -type compound having a highly distorted spinel structure, and of a non-crystalline phase consisting of nearly-pure SiO_2 . The diffusion-controlled formation of γ - Al_2O_3 plus SiO_2 from an ideally homogeneous single-phase precursor requires a phase separation which would be difficult to justify at the low temperature under consideration (800 to 900 °C). Thus our findings support the idea that the precursors are at least partially diphasic with nanometre-sized though highly long-range-disordered Al_2O_3 - and SiO_2 -rich domains. Larger-sized Al_2O_3 -rich domains may occur more in SGM than in CM precursors. This is suggested by the ^{27}Al NMR spectra of SGM material heat-treated at 800 °C, which show the long-range-disordered Al_2O_3 domains to be transformed to γ - Al_2O_3 , while corresponding ^{27}Al spectra of CM still display the characteristic triplet of a starting precursor.

If this interpretation is correct, then on the other hand the lower CM mullite formation temperatures

may be due to more homogeneously distributed and smaller sized Al_2O_3 - and SiO_2 -rich domains with associated shorter diffusion pathways in the CM precursors as compared with SGM material. DTA and TG analyses and MAS NMR spectroscopy do not support the arguments of Pask *et al.* [21] that $\text{AlO}(\text{OH})$ particles embedded in SiO_2 -rich gels exist in the precursors: in $\text{AlO}(\text{OH})$, Al is only sixfold-coordinated while the SGM and CM precursors contain fourfold, (fivefold), and sixfold-coordinated polyhedra. Furthermore, $\text{AlO}(\text{OH})$ should display a dehydration peak in the DTA patterns, which has not been observed.

The transformation of SGM and CM precursors to mullite is basically very similar to the metakaolinite–mullite reaction, and comparable transformation mechanisms may be considered in both cases. Metakaolinite decomposes near 950 °C to a γ - Al_2O_3 -type structure and free silica, plus some minor amount of mullite. Two transformation mechanisms have been envisaged: Brindley and Nakahira [8, 22] and Chakravorty and co-workers [23–25] proposed that metakaolinite decomposes upon heating to an aluminium silica spinel with the composition $\text{Si}_8[\text{Al}_{10.67}\square_{5.33}]\text{O}_{32}$ (where \square is the vacancy) and some excess SiO_2 . A second possibility most thoroughly discussed on the basis of electron density distribution measurements, X-ray spectroscopy and infrared analyses [26–28] suggested the formation of pure γ - Al_2O_3 ($\text{Al}_8[\text{Al}_{13.33}\square_{2.66}\text{O}_{32}]$) plus excess SiO_2 . Our MAS NMR studies, which yielded ^{29}Si spectra having shoulders near – 80 p.p.m., imply that the γ - Al_2O_3 produced by thermal decomposition of SGM and CM precursors is not pure Al_2O_3 but rather contains some Si. However, because of the high amount of SiO_2 -rich phase coexisting with γ - Al_2O_3 , the amount of Si in γ - Al_2O_3 is certainly much smaller than that postulated by Chakravorty and Ghosh [13].

Since mullite crystallization from γ - Al_2O_3 and SiO_2 requires redistribution of Al, Si and O, the transformation rate is most certainly diffusion-controlled. The process should be enhanced by the defect structure of γ - Al_2O_3 . On the other hand, mullitization should be favoured if a topotactical transformation with preservation of structural units is taken into consideration. Actually such a mechanism with the [001] direction of γ - Al_2O_3 lying parallel to the $\langle 110 \rangle$ direction of mullite and partial preservation of the aluminium–oxygen octahedra chains has been discussed in the literature [29–32]. The idea of a partial preservation of the aluminium–oxygen octahedra chains during the γ - Al_2O_3 + SiO_2 to mullite reaction seems to be reasonable, since it agrees with the suggestion that these structural units are the most stable elements of the aluminium silicates andalusite, sillimanite and mullite [32–34].

The observation that the initially formed low-temperature mullites are Al_2O_3 -rich may be explained by their crystallization on γ - Al_2O_3 surfaces [21], while the transformation mechanism discussed by Wei and Holloran [35] is obviously not correct. Due to the high Al_2O_3 content the “orthorhombic character” of the low-temperature mullites is low, and extrapolation

of a and b lattice constants to lower temperatures yields (pseudo-)tetragonal mullite at about 875 °C for mullite SGM and about 750 °C for mullite CM (see Fig. 1 and Reference 36). Lattice parameter measurements and ^{27}Al and ^{29}Si MAS NMR data show that the temperature-induced reaction of unstable, low-temperature Al_2O_3 -rich mullite with the coexisting SiO_2 -rich phase to stable 3/2-type mullite ($3\text{Al}_2\text{O}_3 \cdot 2\text{SiO}_2$) is a gradual process with no measurable enthalpy effect. There is no information on whether the transformation of “ Al_2O_3 -rich” mullite to the stable 3/2-type mullite does proceed through a nanometre-scale mixed-layer state of Al_2O_3 -rich and Al_2O_3 -poor mullite units, or if mixed crystals are formed. High-resolution TEM studies, which could provide more details, are extremely difficult to carry out due to problems related to sample preparation. In any case, similar lattice constants of short-time (15 h) and long-time (120 h) annealing experiments show that the kinetics of the Al_2O_3 -rich to 3/2-type mullite transformation process is essentially controlled by the annealing temperature, whereas the annealing time plays only a minor role.

Acknowledgements

The authors wish to thank H. Krause (Bonn) for performing X-ray diffractograms and Dr T. Ryman-Lipinski (Bonn) for DTA and TG investigations. One of the authors (H.S.) received a research grant from the German Research Foundation (DFG). This is gratefully acknowledged.

References

1. S. SOMIYA, R. F. DAVIS and J. A. PASK (eds), “Mullite and Mullite Matrix Composites”, Ceramic Transactions Vol. 6 *Amer. Ceram. Soc.* (1990) pp. 1–649.
2. G. ENGELHARDT and D. MICHEL, “High-Resolution Solid-State NMR of Silicates and Zeolites” (Wiley, New York, 1987) pp. 143–157.
3. K. OKADA, N. OTSUKA and J. OSSAKA, *J. Amer. Ceram. Soc.* **69** (1986) 251.
4. K. OKADA and N. OTSUKA, *ibid.* **69** (1986) 652.
5. I. M. LOW and R. McPHERSON, *J. Mater. Sci.* **24** (1989) 926.
6. M. YOSHIMURA, Personal Communication (1987).
7. D. W. HOFFMAN, R. ROY and S. KOMARNENI, *J. Amer. Ceram. Soc.* **67** (1984) 468.
8. G. W. BRINDLEY and M. NAKAHIRA, *ibid.* **42** (1959) 311.
9. A. K. CHAKRAVORTY and D. K. GHOSH, *ibid.* **61** (1978) 170.
10. S. H. RISBUD, R. J. KIRKPATRICK, A. P. TAGLIALAVORE and B. MONTEZ, *ibid.* **70** (1987) C-10.
11. J. V. SMITH and C. S. BLACKWELL, *Nature* **303** (1985) 223.
12. I. W. M. BROWN, K. J. D. MACKENZIE, M. E. BOWDEN and R. H. MEINHOLD, *J. Amer. Ceram. Soc.* **68** (1985) 298.
13. A. K. CHAKRAVORTY and D. K. GHOSH, *ibid.* **71** (1988) 978.
14. L. H. MERWIN, A. SEBALD, H. RAGER and H. SCHNEIDER, *Phys. Chem. Min.* **18** (1991) 47.
15. J. ROCHA and J. KLINOWSKI, *ibid.* **17** (1990) 179.
16. J. KLINOWSKI, *Nature* **346** (1990) 509.
17. A. SAMOSON and E. LIPPMAN, *J. Magn. Reson.* **84** (1989) 410.
18. K. T. MÜLLER, B. Q. SUN, G. C. CHINGAS, J. W. ZWANZIGER, T. TERAQ and A. PINES, *ibid.* **86** (1990) 470.
19. Y. WU, B. Q. SUN, A. PINES, A. SAMOSON and E. LIPPMAN, *ibid.* **89** (1990) 297.
20. Y. WU, B. F. CHMELKA, A. PINES, M. E. DAVIS, P. J. GROBET and P. A. JACOBS, *Nature* **346** (1990) 550.
21. J. A. PASK, X. W. ZHANG, A. P. TOMSIA and B. E. YOLDAS, *J. Amer. Ceram. Soc.* **70** (1987) 704.
22. G. W. BRINDLEY and M. NAKAHIRA, *ibid.* **42** (1959) 314.
23. A. K. CHAKRAVORTY and D. K. GHOSH, *ibid.* **60** (1977) 165.
24. *Idem.*, *ibid.* **61** (1978) 90.
25. A. K. CHAKRAVORTY, D. K. GHOSH and P. KUNDU, *ibid.* **69** (1986) C-200.
26. A. J. LEONHARDT, *ibid.* **60** (1977) 37.
27. M. BULENS, A. LEONHARD and B. DELMON, *ibid.* **61** (1978) 81.
28. H. J. PERCIVAL, J. F. DUNCAN and P. K. FOSTER, *ibid.* **57** (1974) 57.
29. J. E. COMOFORO, R. B. FISCHER and W. F. BRADLEY, *ibid.* **31** (1948) 254.
30. G. W. BRINDLEY and M. NAKAHIRA, *ibid.* **42** (1959) 319.
31. J. J. COMER, *ibid.* **43** (1960) 378.
32. H. SCHNEIDER, Habilitationsschrift, Faculty of Chemistry, University of Münster (1985) pp. 1–148.
33. W. GUSE, H. SAALFELD and J. TJANDRA, *N. Jb. Miner. Mh.* (1979) 175–185.
34. W. PANNHORST and H. SCHNEIDER, *Min. Mag.* **42** (1978) 195–198.
35. W.-C. WEI and J. W. HALLORAN, *J. Amer. Ceram. Soc.* **71** (1988) 166–172.
36. H. SCHNEIDER and T. RYMAN-LIPINSKI, *ibid.* **71** (1988) C-162.

Received 10 October 1990
and accepted 20 March 1991